

# Quantifying sleep apnea heterogeneity using hierarchical Bayesian modeling

Glenn Palmer<sup>1</sup> and David B. Dunson<sup>1,2</sup>

<sup>1</sup>Department of Statistical Science, Duke University

<sup>2</sup>Department of Mathematics, Duke University

## Abstract

Obstructive Sleep Apnea (OSA) is a breathing disorder during sleep that affects millions of people worldwide. The diagnosis of OSA often occurs through an overnight polysomnogram (PSG) sleep study that generates a massive amount of physiological data. However, despite the evidence of substantial heterogeneity in the expression and symptoms of OSA, diagnosis and scientific analysis of severity typically focus on a single summary statistic, the Apnea-Hypopnea Index (AHI). To address the limitations inherent in such analyses, we propose a hierarchical Bayesian modeling approach to analyze PSG data. Our approach produces an interpretable vector of random effect parameters for each patient that govern sleep-stage dynamics, rates of OSA events, and impacts of OSA events on subsequent sleep-stage dynamics. We propose a novel approach for using these random effects to produce a Bayes optimal cluster of patients under K-means loss. We use the proposed approach to analyze data from the APPLES study. This analysis produces clinically interesting groups of patients with sleep apnea and a novel finding of an association between OSA expression and cognitive performance that is missed by an AHI-based analysis.

**Keywords**— Sleep monitoring data, hierarchical Bayesian modeling, Markov mixed effects model, time-to-event data, clustering, Bayesian decision theory

## 1 Introduction

Obstructive sleep apnea (OSA) is a widespread breathing disorder characterized by periodic narrowing or obstruction of the pharyngeal airway of a person during sleep, leading to intervals of decreased or stopped

breathing (Osman et al., 2018). Estimates of OSA prevalence in the general population range from 9% to 38%, and are higher for particular subgroups such as men, older adults, and people with obesity (Senaratna et al., 2017). Associations have been found between untreated OSA and health conditions, including metabolic disorders (Drager et al., 2013), cardiovascular disease (Kapur et al., 2008; Walia et al., 2014), and depression (Wheaton et al., 2012). However, despite the potentially severe consequences of OSA and its high prevalence, most people with OSA are not diagnosed (Osman et al., 2018), suggesting that improving the OSA diagnosis process is an important public health issue.

The gold standard for diagnosing OSA is the polysomnogram (PSG), in which a patient spends a night in a sleep lab, and their airflow, respiratory effort, pulse, oxygen saturation, movements, and sleep stages (as indicated by EEG analysis) are recorded (Rundo and Downey III, 2019). These PSG data are analyzed to identify events when a person’s breathing decreased significantly or stopped for at least 10 seconds, referred to as hypopnea or apnea events, depending on their severity. The total count of these events is divided by the total number of hours of sleep to calculate the apnea-hypopnea index (AHI), which is used to diagnose OSA – an AHI above 5 indicates sleep apnea, with higher values interpreted as more severe cases (Rundo and Downey III, 2019). Although the AHI is simple to compute and interpret, it has serious limitations. Osman et al. (2018) note that AHI misses important differences in event severity; a person with low AHI can experience significant effects in terms of oxygen desaturation and clinical symptoms if their apnea events are severe. On the other hand, if a person has a large number of minor events that are not extreme enough to be scored, they could have a misleadingly low AHI compared to the extent to which their breathing truly is disordered (Sankari et al., 2017; Koch et al., 2017). There are other sources of heterogeneity within patients who have a given AHI, such as which stages of sleep the events occur during and how disruptive they were to sleep continuity. Given these factors, studies have often struggled to find meaningful associations between AHI and clinical symptoms (Weaver et al., 2005). Given the time and expense involved in performing PSG studies and the rich datasets they produce, it is critical to obtain more robust, descriptive, and clinically useful measures of OSA.

In this article, we propose an approach to illuminate the relationship between the rate of events of apnea and hypopnea and the dynamics of the sleep stage in people with OSA. There has been recent interest in sleep stage-specific OSA, with some evidence that a high rate of events during rapid eye movement (REM) sleep may be particularly harmful (Aurora et al., 2018; Varga and Mokhlesi, 2019). There is also a great interest in the fraction of time people spend in each stage of sleep, often referred to as sleep architecture (Pase et al., 2023). However, there have been limited approaches to unravel the relationship between the two (Bianchi et al., 2010). We seek to develop a modeling approach that can (1) illuminate population-level variation in sleep stage dynamics and sleep stage-specific OSA, (2) identify individuals whose sleep dynamics

are particularly strongly affected by their apnea and hypopnea events, and (3) evaluate whether the sleep-stage disruptiveness of a case of OSA is associated with other clinical variables, including the severity of symptoms. To do so, we formulate a hierarchical Bayesian model, with patient-level random effects governing the variation in stage-specific event rates and stage-transition probabilities.

## 1.1 Relevant literature

It has been widely acknowledged in the literature on sleep research that there is substantial heterogeneity in patients with OSA that is not represented by a simple AHI-based approach. [Eckert et al. \(2013\)](#) proposed a framework for defining OSA “phenotypes” based on anatomical characteristics and the impact of OSA on breathing patterns and arousal, suggesting that different treatments may be optimal for different phenotypes. [Mokhlesi et al. \(2014\)](#) examined associations between AHI values specific for sleep stages and hypertension, finding that REM AHI greater than 15 was associated with the risk of hypertension, even in patients with a total AHI below 5. [Gagnadoux et al. \(2016\)](#) performed a cluster analysis based on patient demographics and symptoms and found that the effectiveness of CPAP treatment varied between clusters. See [Zinchuk et al. \(2017\)](#) for a clinical review of approaches for OSA phenotyping.

When investigating sleep architecture, simple summary statistics are typically used, such as the total time spent asleep, the amount of time awake after the first onset of sleep, and the amount or fraction of time spent in each sleep stage ([Hermans et al., 2022](#)). However, noting that such summaries may still miss significant variation in dynamics (e.g., a large fraction of REM sleep could result from many short cycles or a small number of long cycles), a relatively small literature has formed proposing approaches to model the sleep stage dynamics directly. These approaches can be broadly categorized into (1) modeling uninterrupted sleep stage durations using methods from survival analysis, and (2) modeling transition probabilities between sleep stages using a Markov model ([Hermans et al., 2022](#)). In the first category, [Norman et al. \(2006\)](#) compared “sleep continuity,” defined as the duration of intervals of sleep between waking up, between healthy participants and those with OSA using Kaplan-Meier curves ([Kaplan and Meier, 1958](#)) and a log-rank test ([Mantel et al., 1966](#)), concluding that the OSA patients had significantly less continuous sleep. [Klerman et al. \(2013\)](#) modeled REM and non-REM uninterrupted durations with an exponential distribution and found that non-REM stability was higher for younger participants. Also modeling REM and non-REM durations with exponential distributions, [Bianchi et al. \(2010\)](#) found that expected continuous durations were shorter in both REM and non-REM sleep for OSA compared to healthy participants. In the second category, [Karlsson et al. \(2000\)](#) treated sleep-stage transitions as Markovian and modeled each possible transition using a mixed-effects logistic regression model, applying this approach to evaluate the effectiveness of temazepam for patients with insomnia. [Bizzotto et al. \(2010\)](#) expanded on this approach, using multinomial logistic

regressions to ensure the estimated transition probabilities from a given stage added up to 1, and [Kjellsson et al. \(2011\)](#) applied this approach to model sleep dynamics in insomnia patients. Finally, [Yetton et al. \(2018\)](#) combined the two types of approaches, modeling sleep stage durations separately from Markovian transition probabilities that excluded self-transitions, using a Bayesian network approach to evaluate how durations and transition probabilities varied by categorical covariates.

## 1.2 Our contribution

The above literature conveys a broad recognition of substantial heterogeneity among OSA patients, including their sleep dynamics, which is not captured by AHI. However, to our knowledge, no one has presented an approach to model the variability of sleep dynamics jointly with the occurrence of OSA events. In particular, existing modeling approaches do not allow the probability of a sleep transition to depend on the occurrence of a recent apnea event. We propose an approach that not only achieves these goals, but also quantifies patient-level heterogeneity in sleep-stage dynamics, in sleep-stage specific rates of OSA events, and critically, in the level of disruptiveness of a patients’ OSA events to their sleep-stage dynamics. We then propose an approach for inferring groups of patients with similar random effects that is Bayes optimal under K-means loss. Our full approach illuminates previously unexplored variation in OSA severity. In doing so, we establish a new framework for modeling OSA heterogeneity that can be applied to numerous cohorts of patients.

In Section 2, we give more information on the motivating application and the data set. In Section 3, we describe our modeling approach. In Section 4, we demonstrate the efficacy of our model in simulations. In Section 5, we present our data analysis results. Section 6 presents some discussion and future directions.

# 2 Polysomnogram data analysis

## 2.1 Background

The Apnea Positive Pressure Long-term Efficacy Study (APPLES) was a multicenter study of the efficacy of continuous positive airway pressure (CPAP) in improving neurocognitive function in OSA patients ([Kushida et al., 2006](#)). APPLES enrolled 1204 participants, which they randomized into CPAP treatment and control groups and followed for six months. Baseline PSG data measured at each participant’s diagnostic visit is available through the National Sleep Research Resource ([Zhang et al., 2018](#)) for 1104 of these participants, as well as demographic covariates, results of neurocognitive testing, and summaries of follow-up appointments ([Quan et al., 2011](#)).

The primary outcomes with measurements at the diagnostic visit in APPLES were two neurocognitive tests – the Pathfinder Number Test ([Partington and Leiter, 1949](#)) and the Buschke Verbal Selective Remind-

ing Test (BSRT) (Buschke, 1973). In Pathfinder, participants try to select consecutive numbers displayed in boxes in different quadrants of a computer screen. The Pathfinder is designed to assess attention and psychomotor function, and the primary measured outcome is the time a participant takes to complete the test, up to 60 seconds (Quan et al., 2011). In the BSRT, participants are presented with a list of 12 unrelated words and then asked to recall as many of them as possible over the course of 6 trials. The BSRT is designed to assess verbal learning and short- and long-term memory, and the primary measured outcome is the total number of words correctly recalled over the 6 trials, ranging up to all 72 words (Quan et al., 2011). In their analysis of these test results, Quan et al. (2011) performed hypothesis tests comparing Pathfinder and BSRT scores for participants with baseline AHI values below 10 to those of patients with AHI values above 50. In both cases, they found that high-AHI patients performed worse. However, they then fit subsequent regression models that also accounted for demographic characteristics, and the associations between the tests and AHI were no longer significant in these multivariate models. These results correspond to the general state of the literature, in that there are examples of studies that find associations between OSA and neurocognitive outcomes (e.g., Jokic et al. (1999) found that Pathfinder scores improved in patients after OSA treatment), but in general the results have been mixed, with other studies not finding associations with cognitive outcomes (Weaver et al., 2005).

In this work, we postulate that associations between the rate of OSA events and neurocognitive outcomes may vary by how disruptive a particular patient’s events are to their sleep dynamics. This corresponds to the increasing focus on personalized approaches to medicine (Mathur and Sutton, 2017), which has been suggested to be critical for understanding and quantifying OSA (Edwards et al., 2019). To investigate this possible patient heterogeneity, we propose a hierarchical Bayesian approach to quantify patient-level OSA disruptiveness, and apply it to re-analyze the APPLES baseline PSG data.

## 2.2 Data description and preprocessing

The released APPLES data set included PSG data for 1104 participants, selected based on being at least 18 years old and having a clinical diagnosis of OSA, but never having used a CPAP before. Other exclusion criteria can be found in Kushida et al. (2006), and include a number of medical conditions, medications, and a history of a sleepiness-related motor vehicle accident (Quan et al., 2011). After enrollment, the participants attended a diagnostic visit, where the PSG was measured between 7 and 9 hours, followed by a day of neurocognitive testing and monitoring. For PSG, sleep stages were manually recorded for 30-second intervals referred to as epochs using the Rechtschaffen and Kales criteria (Rechtschaffen and Kales, 1968), categorized into awake, REM sleep, and three levels of non-REM sleep numbered by depth. Apnea events were defined by a decrease of at least 90% from the baseline nasal pressure amplitude for an interval of at

least 10 seconds. Hypopnea events were defined as a 10-second or longer decrease in nasal pressure between 50% and 90%, or a decrease less than 50% that was also accompanied by a 3% or greater oxygen desaturation or arousal, according to (AASM, 1999). The apnea hypopnea index (AHI) was calculated as the total number of apnea and hypopnea events divided by the total hours of sleep.

Before analysis, we removed nine patients who never entered REM sleep, as they likely had unusually poor sleep during the testing procedure. We removed an additional two patients whose recorded sleep stages had inconsistencies in the files for their PSG data, leaving 1093 patients for our primary analysis. In our follow-up analyses of the Pathfinder and BSRT tests, two and one participants were missing these scores, respectively, and therefore were excluded from the corresponding second-stage analysis only.

### 3 Model

#### 3.1 Model description

Consider  $n$  patients, each monitored for a single night of sleep. Let  $s_{ij} \in \{1, 2, 3\} \equiv \{\text{Awake, REM, non-REM}\}$  be the sleep stage for the  $i^{\text{th}}$  patient during the  $j^{\text{th}}$  epoch, where  $j \in \{1, \dots, m_i\}$ . For  $s_{ij} \in \{2, 3\}$ , we model the transition probabilities for  $s_{i,j+1} \in \{1, 2, 3\}$  using a mixed effects multinomial logistic regression model,

$$Pr(s_{i,j+1} = k_n | s_{ij} = k_o) = \frac{\exp(\delta_{ij k_o k_n})}{\sum_{k'_n} \exp(\delta_{ij k_o k'_n})}$$

with

$$\delta_{ij k_o k_n} = \begin{cases} \mu_{k_o k_n} + \gamma_{i k_o k_n} + (\tau_{k_o k_n} + \alpha_{i k_o k_n}) \cdot v_{ij} & \text{if } k_o \neq k_n \\ 0 & \text{if } k_o = k_n \end{cases}$$

where  $v_{ij} = \mathbb{1}(\text{patient } i \text{ has event during epoch } j)$ , and  $\gamma_{i k_o k_n}$  and  $\alpha_{i k_o k_n}$  are random effects, which we expand upon shortly. To facilitate computation, we can write the above model as a multinomial distribution for the associated transition counts. In particular, we let

$$c_{i h k_o} \sim \text{Mult}(\pi_{i h k_o A}, \pi_{i h k_o R}, \pi_{i h k_o N}, n_{i h k_o})$$

where  $c_{i h k_o} \in \mathbb{R}^3$  is the vector of counts of transitions from stage  $k_o$  to each of stage Awake, REM, and non-REM for patient  $i$  during epochs for which  $v_{ij} = h$ . In the above,  $n_{i h k_o}$  is the number of epochs the patient  $i$  spends in the sleep stage  $k_o$  with the status of the event  $h$ , excluding the final recorded epoch, and  $\pi_{i h k_o k_n} = Pr(s_{i,j+1} = k_n | s_{ij} = k_o, v_{ij} = h)$ .

Jointly with the above, we model the inter-event times between apnea/hypopnea events (that is to say,

between the end of one event and the start of the next) using a mixed effects Poisson process for each sleep stage (REM and non-REM). Letting  $w_{ilk}$  be the  $l$ th inter-event time for patient  $i$  during the sleep stage  $k$ , we let

$$w_{ilk} \sim \text{Exp}(\lambda_k \exp(\phi_{ik}))$$

where  $\phi_{ik}$  is a patient-level random effect capturing variability in the event rates for the sleep stage  $k$ . Similarly to our collapsing the sleep-stage transitions into multinomial counts, here we can express the likelihood for the inter-event times in terms of a Poisson distribution for the counts of events in each stage. That is,

$$v_{ik} \sim \text{Poisson}(t_{ik} \lambda_k \exp(\phi_{ik}))$$

where  $v_{ik}$  is the number of events patient  $i$  experiences in sleep stage  $k$ , and  $t_{ik}$  is the time in seconds patient  $i$  spends in sleep stage  $k$ , excluding intervals when they were actively having an event.

Given the above, we have defined ten random effects for each patient:

$$\begin{aligned} \theta_i &= (\gamma_i, \alpha_i, \phi_i)^T \\ &= (\gamma_{iRA}, \gamma_{iRN}, \gamma_{iNA}, \gamma_{iNR}, \alpha_{iRA}, \alpha_{iRN}, \alpha_{iNA}, \alpha_{iNR}, \phi_{iR}, \phi_{iN})^T \in \mathbb{R}^{10}. \end{aligned}$$

We assign the vector  $\theta_i$  a multivariate normal distribution

$$\theta_i \sim N_{10}(0, \Sigma),$$

where we learn  $\Sigma$  using a latent factor model. That is, we let

$$\theta_i = \Lambda \eta_i + \varepsilon_i,$$

$$\eta_i \sim N_k(0, I), \quad \varepsilon_i \sim N_{10}(0, \Omega)$$

where  $\Lambda \in \mathbb{R}^{10 \times k}$  is an unknown factor loadings matrix and  $\Omega = \text{diag}(\omega_1^2, \dots, \omega_{10}^2)$ . This induces the covariance model

$$\theta_i \sim N_{10}(0, \Lambda \Lambda^T + \Omega).$$

By choosing  $k < p$ , this approach allows us to reduce the number of parameters needed to estimate  $\Sigma$  from  $p(p+1)/2$  for a general covariance matrix to  $p(k+1)$ . In addition, while  $\Lambda$  and  $\eta_i$  are in general not identifiable in the above, using the MatchAlign procedure of [Poworoznek et al. \(2021\)](#) we can examine posterior summaries of the  $k$  columns of  $\Lambda$ , which can be thought of as describing low-dimensional components

of  $\theta_1, \dots, \theta_n$ , similar to principal component vectors, but without the restriction that they are orthogonal.

### 3.2 Prior distributions and implementation details

To complete our Bayesian model specification, we assign prior distributions for all parameters. We give gamma priors to the  $\lambda_k$ s, normal priors to the  $\mu_k$ s and  $\tau_k$ s, independent normal priors to all elements of  $\Lambda$ , and inverse-gamma priors to the diagonal elements of  $\Omega$ . To sample from the posterior distribution, we implemented the model using the probabilistic programming language Stan (Carpenter et al., 2017). The code implementing our approach can be found in the online supplement.

### 3.3 Loss-based clustering by $\theta_i$

After fitting our model, we would like to summarize clinically interesting subgroups of patients with similar expressions of OSA captured by their random effects vectors  $\theta_i$ . That is, we would like to estimate a partition  $C = \{C_1, \dots, C_K\}$  of patient indices  $\{1, \dots, n\}$  into  $K$  clusters based on  $\theta_1, \dots, \theta_n$ . Equivalently, we can frame the problem as choosing a vector of  $n$  cluster labels  $c = (c_1, \dots, c_n)$  where each  $c_i \in \{1, \dots, K\}$ . A typical way to infer  $c$  is to model  $\theta_1, \dots, \theta_n$  as arising from a mixture of Gaussian distributions, rather than the single multivariate Gaussian we assigned in Section 3.1. However, such an approach leads to substantial computational hurdles and assumes the existence of distinct groups with Gaussian-distributed data. To avoid these issues, we develop a Bayesian decision-theoretic approach to infer Bayesian clustering estimates based on the posterior samples of the random effect values of patients  $\{\theta_i\}$ . For simplicity and interpretability, we choose the K-means loss function, which minimizes the within-cluster sum of squares (Lloyd, 1982). In Section 3.3.1, we describe an approach for estimating Bayes optimal clustering and cluster centers with K-means loss. Then, in Section 3.3.2, we propose a practical and intuitive notion of uncertainty quantification that is easy to propagate forward in subsequent model summaries.

#### 3.3.1 Point estimation

Accounting for posterior uncertainty in inferring the random effects for each patient, our Bayesian estimator of the clustering and cluster centers corresponds to minimizing the expected k-means loss over  $\pi_{post}$ :

$$\left(\hat{c}, \hat{b}\right) = \arg \min_{c:|C|=K, b \in \mathbb{R}^{K \times d}} \sum_{k=1}^K \sum_{i \in C_k} \mathbb{E}_{\pi_{post}} \left[ \|\theta_i - b_k\|^2 \right]. \quad (1)$$

When applying K-means clustering to observed data rather than uncertain parameters, the problem is often framed as optimizing only over  $c$ , with centers  $b_1, \dots, b_K$  automatically defined as the means of observations

in clusters  $1, \dots, K$ . Adapting such a formulation to our case produces

$$\hat{c}' = \arg \min_{c:|C|=K} \sum_{k=1}^K \sum_{i \in C_k} \mathbb{E}_{\pi_{post}} [|\theta_i - \bar{\theta}_k|^2], \quad (2)$$

where each cluster center  $\bar{\theta}_k$  is a random variable that varies over posterior samples. Note that (1) and (2) are not equivalent and, in general, the learned partitions defined by  $\hat{c}$  and  $\hat{c}'$  will differ. In the results that follow, we focus on the formulation (1); we are interested in interpreting the cluster summaries in the context of the estimated cluster centers, so it is appealing to obtain a principled point estimate of these centers jointly with the assignments. If we first compute  $\hat{c}'$  using (2) and then summarize the centers  $\hat{b}'$  as posterior means conditional on  $\hat{c}'$ , we produce a suboptimal solution  $(\hat{c}', \hat{b}')$  with respect to (1). However, we also implement formulation (2) for comparison and summarize the results in Supplementary Information.

In addition to its interpretability, the formulation (1) is easy to compute, as implied by Proposition 3.1.

**Proposition 3.1.** *Let  $(\hat{c}, \hat{b})$  be the solution to (1). Then we can equivalently compute*

$$(\hat{c}, \hat{b}) = \arg \min_{c:|C|=K, b \in \mathbb{R}^{K \times d}} \sum_{k=1}^K \sum_{i \in C_k} \|\mathbb{E}_{\pi_{post}}[\theta_i] - b_k\|^2.$$

*That is, we can simply apply the standard K-means algorithm to the posterior means of  $\theta_1, \dots, \theta_n$ .*

The proof of Proposition 3.1 is straightforward and is given in the Appendix. With the efficiency of modern implementations of K-means, such as the `kmeans` function in R (R Core Team, 2023), this result suggests that finding the Bayes-optimal clustering is computationally trivial. By choosing the number of posterior samples  $m$  to be large, we can estimate  $\mathbb{E}_{\pi_{post}}[\theta_i]$  arbitrarily well with Monte Carlo sample averages.

### 3.3.2 Uncertainty quantification

To characterize uncertainty in clustering patients into groups, we focus on the conditional posterior probability of assigning patient  $i$  to cluster  $k$  treating the cluster centers as fixed at  $\hat{b}$ :

$$Pr(c_i = k | b = \hat{b}) = \mathbb{E}_{\pi_{post}} \left[ \mathbb{1} \left( \arg \min_{k' \in \{1, \dots, K\}} \|\theta_i - \hat{b}_{k'}\|^2 = k \right) \right]. \quad (3)$$

A Monte Carlo estimate of the probabilities in (3) can be easily calculated with posterior samples, and these probabilities can then be propagated through to account for uncertainty in any future patient summaries based on cluster assignment.

We purposely avoid accounting for uncertainty in inferring the cluster centers. Fixing the centers gives a clear interpretation of statements such as “patient  $i$  is in cluster  $k$  with probability  $p$ ” that would be

muddled if the location of the cluster  $k$  was also in question. In addition, we are interested in summarizing clinically interesting groups of our  $n$  patients without assuming true, well-separated patient clusters. Given this goal, it is reasonable to fix the locations of these group of patients according to (1) and then examine the uncertainty relative to these locations. Thus, our results in Section 5 account only for the uncertainty in (3). Two alternative approaches are described and implemented in the Supplementary Information.

## 4 Simulations

To evaluate our approach, we simulated PSG data in three scenarios. In Scenario 1, we generated data from our model as specified. For each replication, we drew  $\mu$  parameters independently from a Uniform $[-4, -2]$  distribution,  $\tau$  from Uniform $[0, 1]$ ,  $\lambda$  from Uniform $[0.01, 0.03]$ , and two additional parameters  $\mu_{AR}$  and  $\mu_{AN}$  that govern transitions from Awake from Uniform $[-3, -1]$ . We generate a factor model covariance for random effects with  $k = 3$  factors. Factor loadings were drawn independently from  $N(0, 0.2)$  distributions, and idiosyncratic variances were set to 0.2. The random effects  $\theta_i$  were then drawn from the resulting multivariate normal distribution. In Scenario 2, we used the same setup, except that the parameters  $\mu$  and  $\lambda$  were allowed to vary over time, so that the baseline rates of stage transitions and OSA events were not constant over the course of the night. We drew  $\mu$  parameters as linear functions with intercepts from Uniform $[-4, -3]$  and slopes from Uniform $[-0.001, 0.001]$  in units of epochs, so that over a 1000-epoch night, a given parameter could shift by up to one unit. We drew  $\lambda$  intercepts from Uniform $[0.01, 0.03]$  and slopes from Uniform $[-0.00001, 0.00001]$ , for a total shift of up to 0.01. In Scenario 3, we generate fixed effects as in Scenario 1, but draw random effects  $\theta_i$  from a mixture of normals. The component centers were drawn independently from  $N_{10}(0, 0.25I)$ , the patients were assigned uniformly at random to one of the four groups, and then the values  $\theta_i$  were drawn from a multivariate Gaussian with the appropriate mean and variance  $0.25I$ . For identifiability, we then center the  $\theta_i$  values on mean zero. For each scenario and each of 100 random initializations, we generated one night of data for each of 1000 patients, with each night recorded for 1000 epochs including any awake intervals; this corresponds to eight hours and twenty minutes of recording for each patient.

A summary of our model’s accuracy is shown in Table 1, averaged over 100 replications. Accuracy is similar across the three scenarios. Coverage of 95% credible intervals is excellent for fixed effects, random effects, and elements of the random effect covariance matrix across the board, with only slight differences between the different data-generating processes. For the random effects and their covariance, which are focal points of our applied results, mean squared error does not suffer substantially given non-constant fixed effects in Scenario 2, and the covariance 95% interval coverage actually improves slightly compared to Scenario 1 where our model is correctly specified. It is somewhat more difficult to interpret comparisons in random effect

MSE for Scenario 3, since the random effects are drawn from a mixture that likely has a somewhat different scale than the factor model covariance, but in general performance is good, with the smallest MSE and excellent coverage for the random effects, as well as smaller MSE and improved coverage for the fixed effects, which are generated identically to those in Scenario 1. Overall, these results suggest that our inferences are reasonably robust to misspecification, both in terms of non-constant dynamics and event rates, and in terms of substantial misspecification of the random effects distribution.

	Scenario 1	Scenario 2	Scenario 3
Fixed Effect MSE	0.00101	N/A	0.000482
Fixed Effect Coverage	0.943	N/A	0.985
Random Effect Covariance MSE	0.00159	0.00163	N/A
Random Effect Covariance Coverage	0.945	0.953	N/A
Random Effect MSE	0.107	0.120	0.0993
Random Effect Coverage	0.949	0.948	0.951

Table 1: Accuracy of parameter estimates under three data generation scenarios. In scenario 1 the model is correctly specified, while in scenarios 2 and 3 there are different types of misspecification.

Finally, to evaluate the efficacy of our clustering approach, for Scenario 3 data, we additionally generated an outcome variable for each patient from a mixture distribution with the same assignments as the mixture for  $\theta_i$ . The means for these components were chosen without replacement from  $\{1, 2, 3, 4\}$ , and then the patients' values were drawn with Gaussian noise with standard deviation 0.2. We then clustered patients in two ways, first with our K-means approach using their estimated  $\hat{\theta}_i$  values, and then for comparison, using K-means with standardized values of REM AHI, non-REM AHI, total time in REM, and total time in non-REM as input data. These represent simple summary statistics, often used to infer stage-specific event rates and sleep architecture. Table 2 compares the adjusted Rand index for each clustering compared to the true mixture components averaged over 100 replications. Our approach has a dramatically better clustering accuracy, with an ARI of  $\sim 0.7$ , compared to a poor ARI of  $\sim 0.2$  for the competitor. The competitor finds bigger clusters on average, as the within-cluster outcome variance is over double that for our approach.

	K-means with $\hat{\theta}_i$	K-means with basic summaries
Adjusted Rand Index	0.670	0.229
Within-cluster outcome variance	0.447	0.959

Table 2: Accuracy of clustering based on  $\hat{\theta}_i$  compared to using patient summaries of REM AHI, non-REM AHI, time in REM, and time in non-REM, evaluated on Scenario 3 simulated data.

## 5 Application

### 5.1 Exploratory data analysis

Before fitting our model, we performed some data visualization to get a sense of the heterogeneity in OSA event occurrence in the APPLES participants. Figure 1 shows the distribution of AHI values, both in general, as used when classifying OSA severity, and specifically during REM and non-REM sleep. Observe that the average AHI appears to be somewhat higher during REM sleep compared to non-REM sleep.

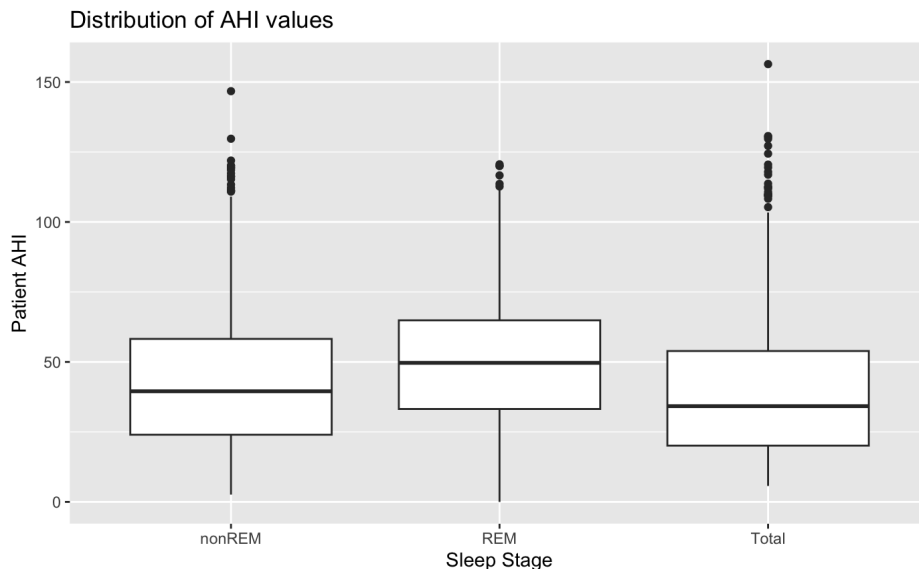


Figure 1: Distribution of REM, non-REM, and overall AHI values for patients in the APPLES study.

To provide additional context to the AHI distributions, Figure 2 shows the distributions of the average event durations at the patient level during non-REM and REM sleep. Here again, the event durations appear longer on average in REM sleep compared to non-REM sleep. This not only adds to the evidence that OSA intensity may be higher for the average person in REM sleep compared to non-REM, but actually suggests that the difference between AHI values in REM vs. non-REM may in some sense understate the higher rate during REM sleep, since longer average events lead to a lower AHI given the same distribution of times between events. (E.g., a patient with two 10-second events each minute will have double the AHI of a patient with one 40-second event each minute, even though they both have an average inter-event time of 20 seconds, and more of the second patient’s sleep time is spent having events.) This suggests our approach of modeling inter-event times as the time between the end of one event and the start of the next may more reasonably capture the difference in in OSA intensity compared to AHI.

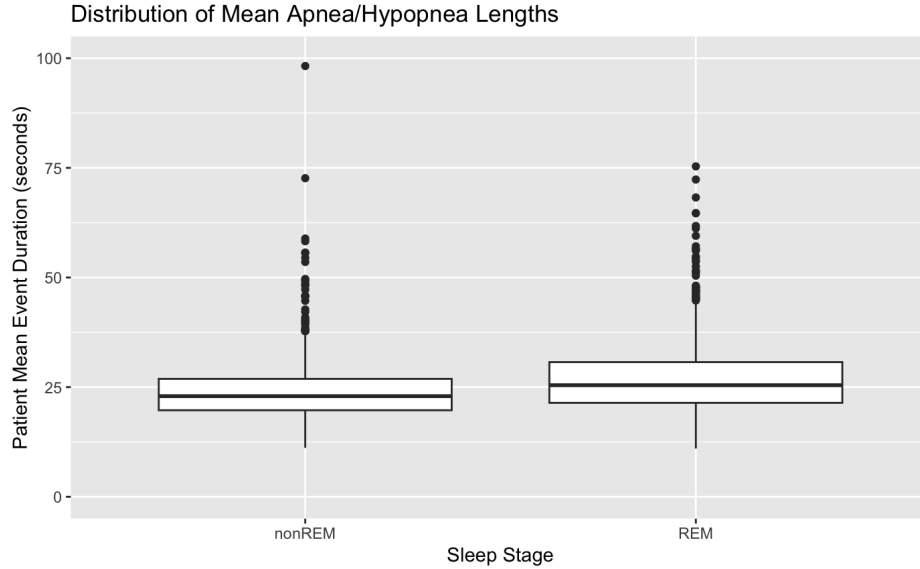


Figure 2: Distribution of average hypopnea/apnea event durations for patients in the APPLES study. Four patients are omitted for REM sleep: two with zero events during REM, and two with outlier mean event lengths of 219 and 188 seconds.

Finally, Figure 3 shows the distributions of time spent in REM vs. non-REM sleep in the sample of patients. Clearly, the average patient spends far more time in non-REM than in REM. This suggests that sleep stage-specific event rates can affect sleep quality and health through different pathways. On the one hand, since non-REM represents the majority of sleep, an elevated rate of non-REM events has a larger impact on the total number of events in a night than an elevated REM rate, as reflected by the similarity in the non-REM and overall AHI distributions in Figure 1. Thus, one can imagine that the rate during non-REM could be particularly impactful on certain health outcomes of interest. However, since REM sleep is believed to be particularly important for learning and memory (Peever and Fuller, 2017), if an elevated rate of REM events causes a patient’s small but important amount of REM sleep to be interrupted or cut short, this could also be highly detrimental.

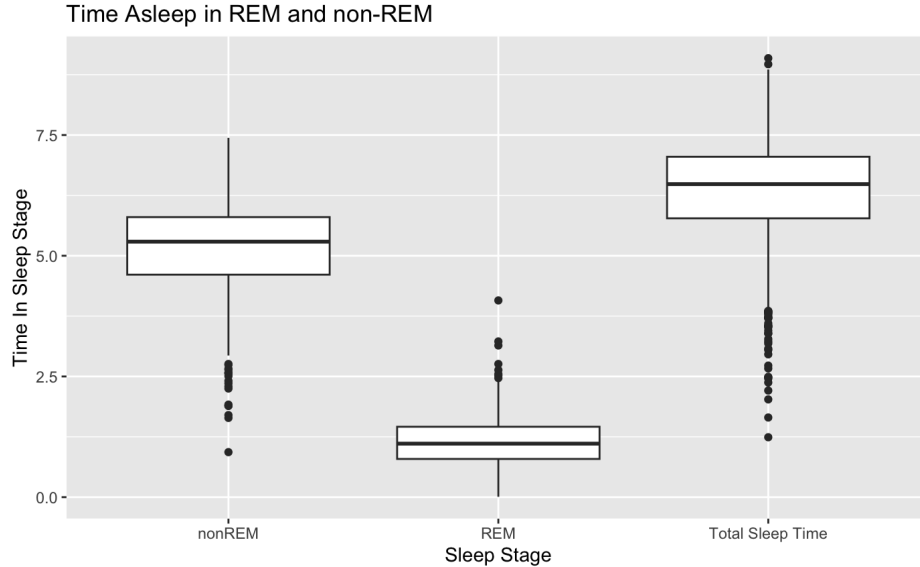


Figure 3: Distributions of time in non-REM sleep, time in REM sleep, and total time asleep for patients in the APPLES study.

## 5.2 Model fitting

To sample from the posterior, we implemented our model in the probabilistic programming language Stan (Carpenter et al., 2017). We ran four chains, each for 2500 burn-in iterations and 2500 subsequent posterior samples, for a total of 10,000 posterior samples. To choose the number of factors  $k$  in the factor model for random effects, we ran a principal component analysis on the estimated random effect vectors in a simpler model with diagonal covariance, and examined the scree plot; this resulted in a choice of  $k = 5$ . The mixing appears satisfactory, with all effective sample sizes larger than 2700 and all Gelman-Rubin diagnostic values less than 1.02 in all main effects, random effects, and random effect covariance terms.

To evaluate the quality of model fit, we performed several posterior predictive checks. To simulate a night’s data for each patient and each posterior sample, we simulated sleep stage transitions and OSA event occurrences conditional on the person’s total number of epochs asleep. If a person transitioned to Awake, we draw the next sleep stage uniformly at random from that patient’s observed initial sleep stages after waking up. To generate the duration of events, we draw the duration of events uniformly at random from the patient’s list of event durations for the current sleep stage. Figure 4 shows the posterior predictive means (orange dots) and 95% intervals (blue lines) for the amount of time spent in non-REM sleep and the number of total OSA events occurring during non-REM sleep. The black dots indicate the observed value for each patient. The intervals contain the observed values for 99.9% of the patients for time spent in non-REM and 99.8% of the patients for the count of non-REM events. The results are similar for REM sleep, with 95% interval coverage of 99.9% and 98.9%. The posterior predictive plots for time and event count in REM as well

as posterior predictive AHI values in REM and non-REM are presented in the Supplementary Information.

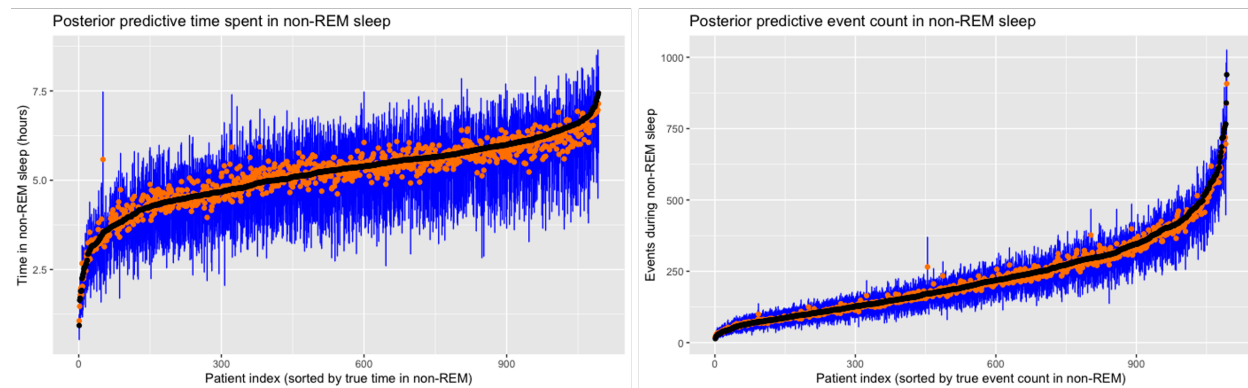


Figure 4: Posterior predictive distributions of time spent in non-REM sleep (left) and the number of events occurring during non-REM sleep (right). Black dots are observed values; orange dots are posterior predictive means; blue lines are 95% posterior predictive intervals.

## 5.3 Posterior summaries

### 5.3.1 Model parameters

Figures 5-6 summarize the posterior distributions for the transition and inter-event model parameters. In the left panel of Figure 5, observe that the posteriors of all  $\mu$  parameters are strongly negative, indicating that for both REM and non-REM sleep, patients are overwhelmingly likely to stay in the same stage from one epoch to the next. The 95% posterior credible intervals for  $\tau_{RN}$ ,  $\tau_{RA}$ ,  $\tau_{NR}$ , and  $\tau_{NA}$  are all strictly positive, indicating that having an apnea event in a given epoch makes the average patient more likely to transition out of their current sleep stage. Note that  $\tau_{RA}$  and  $\tau_{NA}$  have magnitudes larger than  $\tau_{RN}$  and  $\tau_{NR}$ , respectively, indicating that apnea events have a particularly strong effect on the probability of awakening. In the right panel of Figure 5, note that the baseline transition parameters  $\gamma$  appear to have a larger variance for transitions out of REM than for transitions out of non-REM, while the opposite is true for the parameters  $\alpha$ . This suggests that there may be more baseline patient variation in transitions from REM sleep, but more variation in the effect of OSA events during non-REM sleep.

As expected from our EDA in Section 5.1, the left panel of Figure 6 shows that the baseline rate of events is substantially higher during REM sleep compared to non-REM. The random effect variances shown in the right panel of Figure 6 are very similar between REM and non-REM, with the posterior mean slightly higher for non-REM. However, since these random effects  $\phi_{ik}$  affect patient-level expected interevent times multiplicatively, the actual patient-level variability is higher during REM sleep than non-REM, due to the higher baseline rate during REM. Finally, note that given the model setup from Section 3.1, the variances observed for the  $\phi_{ik}$ s indicate substantial patient variation in interevent times. If we take each of the  $\phi_{ik}$

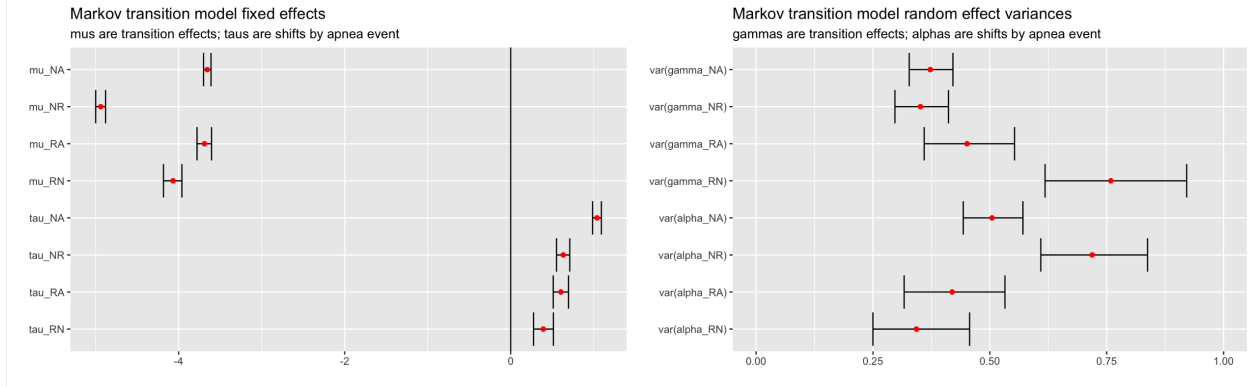


Figure 5: Posterior summaries of fixed effects (left) and random effect variances (right) from the stage transition Markov model. Dots represent posterior means, and intervals represent 95% posterior credible intervals.

variances to be about 0.7, this corresponds to a patient with a rate one standard deviation above the mean having an expected interevent time over five times shorter than a patient whose rate is one standard deviation below the mean.

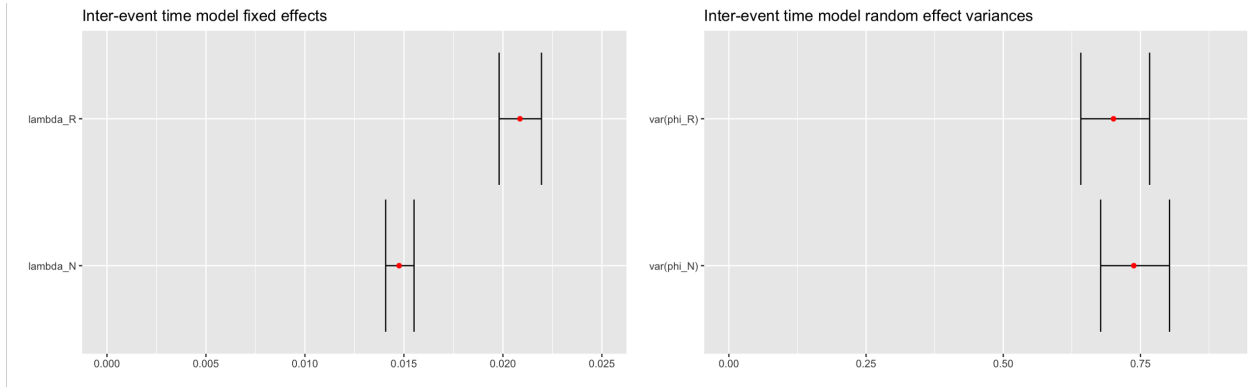


Figure 6: Posterior summaries of fixed effects (left) and random effect variances (right) from the apnea and hypopnea inter-event time model. Dots represent posterior means, and intervals represent 95% posterior credible intervals.

To illustrate the relationships among random effects at the patient level, Figure 7 shows the posterior mean of the correlation matrix for  $\theta_i$ , which provides a number of insights into the patient distribution. First, observe that most correlations between dynamics parameters  $\gamma$  and  $\alpha$  are positive, and that this is particularly true among parameters regarding transitions from REM sleep, suggesting that individuals who are likely to transition out of REM sleep at baseline are also more disrupted than average by OSA events during REM. However, for non-REM parameters, note the negative correlations between  $\gamma_{NR}$  and  $\alpha_{NR}$ , and between  $\gamma_{NA}$  and  $\alpha_{NA}$ , suggesting that patients with high baseline rates of transitions from non-REM sleep tend to experience a smaller disruption than average due to non-REM event occurrences. However, this may be due in part to the logit scale in our model, which implies that the interpretation of  $\alpha_{NA}$  and  $\alpha_{NR}$

depends on the values of  $\gamma_{NA}$  and  $\gamma_{NR}$ . Finally, as expected, the random effects between events  $\phi_R$  and  $\phi_N$  are positively correlated, suggesting that patients with a high rate of OSA events in one REM or non-REM sleep are more likely to also have a high rate in the other. The interpretation of the relationship between these parameters  $\phi$  and the dynamic random effects is more subtle, with a number of moderate positive and negative correlations. However, it is interesting to observe the negative correlations between  $\phi_R$  and  $\alpha_{RA}$ , and between  $\phi_N$  and  $\alpha_{NA}$ , which suggest that patients with a higher rate of OSA events may tend to have their sleep less disrupted by each event.

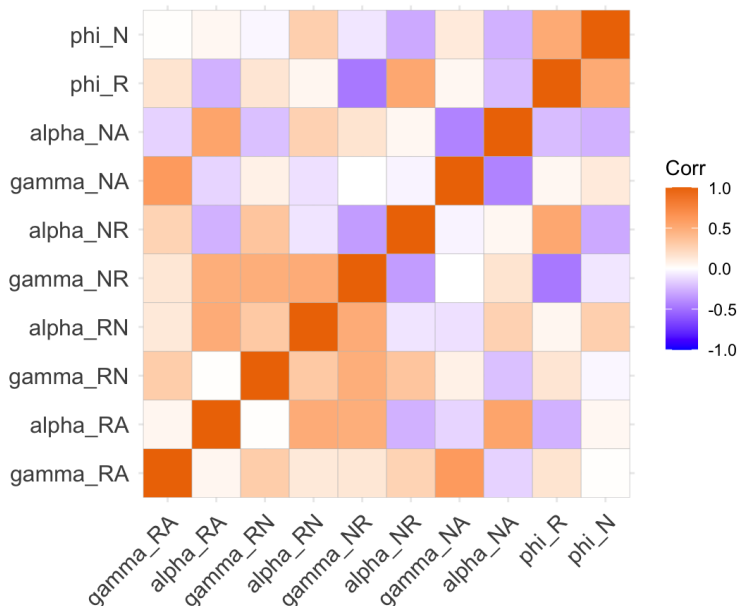


Figure 7: Posterior mean correlation matrix for the random effect vectors  $\theta_i$ .

Figure 8 shows the posterior means of the factor loadings in the matrix  $\Lambda$ , aligned for interpretability using the method of Poworoznek et al. (2021). In general, the interpretations of these factors yield similar insights to examining the correlations in Figure 7. Factors 1 and 5 yield the positive correlations among the REM transition parameters, factor 4 yields the positive correlation between  $\phi_R$  and  $\phi_N$ , and factors 2 and 3 are primarily responsible for the negative correlations discussed above.

### 5.3.2 Clustering

Given the posterior samples of  $\theta_i$ , we computed point estimates of the k-means cluster assignments and centers from (1), as well as the associated assignment probabilities from (3). Letting the number of clusters  $k = 4$ , the estimated centers are shown in Table 3. One way to interpret these centers in terms of sleep and OSA characteristics is to consider whether the  $\gamma$  and  $\alpha$  parameters tend to be high or low, suggesting highly disrupted vs. steady sleep, and whether each of  $\phi_R$  and  $\phi_N$  are high or low. Using this framework, we find

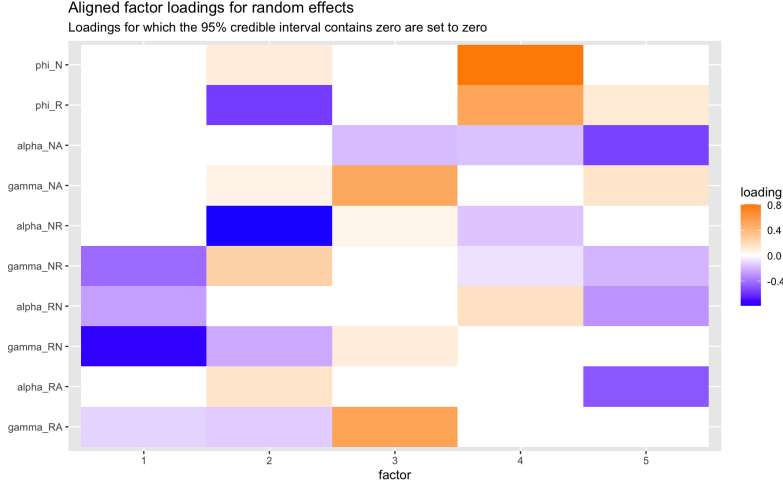


Figure 8: Posterior mean factor loadings after alignment with the procedure of [Poworoznek et al. \(2021\)](#). Loadings for which the 95% credible interval contains zero have been set to zero.

that cluster 1 (276 patients) has moderate sleep dynamics, a low event rate in REM sleep, and a moderate event rate in non-REM sleep, cluster 2 (143 patients) has highly disrupted sleep dynamics with moderate REM and non-REM event rates, cluster 3 (326 patients) has fairly calm sleep dynamics, a moderate event rate in REM, and a low event rate in non-REM, and cluster 4 (348 patients) has fairly calm sleep dynamics but high event rates in both REM and non-REM.

	gamma_RA	gamma_NA	alpha_RA	alpha_NA	gamma_RN	gamma_NR	alpha_RN	alpha_NR	phi_R	phi_N
Cluster 1	-0.17	0.00	0.30	0.17	-0.37	0.31	0.02	-0.86	-0.97	-0.14
Cluster 2	0.62	0.18	0.38	0.08	1.29	0.64	0.61	0.53	0.18	-0.03
Cluster 3	-0.11	-0.19	-0.20	0.16	-0.09	-0.21	-0.26	0.51	-0.01	-0.73
Cluster 4	-0.02	0.10	-0.20	-0.31	-0.16	-0.31	-0.02	-0.02	0.69	0.79

Table 3: Bayes-optimal cluster center estimates based on k-means loss with  $k = 4$ .

The cluster assignment point estimates are shown in Figure 9, indicated by colored points showing each  $\theta_i$  projected into two dimensions. The vertical axis is simply  $\phi_R$ , while the horizontal axis is the first principal component score for PCA performed on the posterior means of  $(\gamma_{RA}, \gamma_{NA}, \alpha_{RA}, \alpha_{NA}, \gamma_{RN}, \gamma_{NR}, \alpha_{RN}, \alpha_{NR})$ . The vector of the first associated principal component is  $(0.28, 0.06, 0.48, 0.23, 0.33, 0.50, 0.52, -0.07)$ , suggesting that a positive value of pc1 roughly corresponds to more disruption of the sleep stages, both at baseline and due to OSA events. Given this interpretation, the projected locations of the clusters appear to correspond to the above interpretation of their centers.

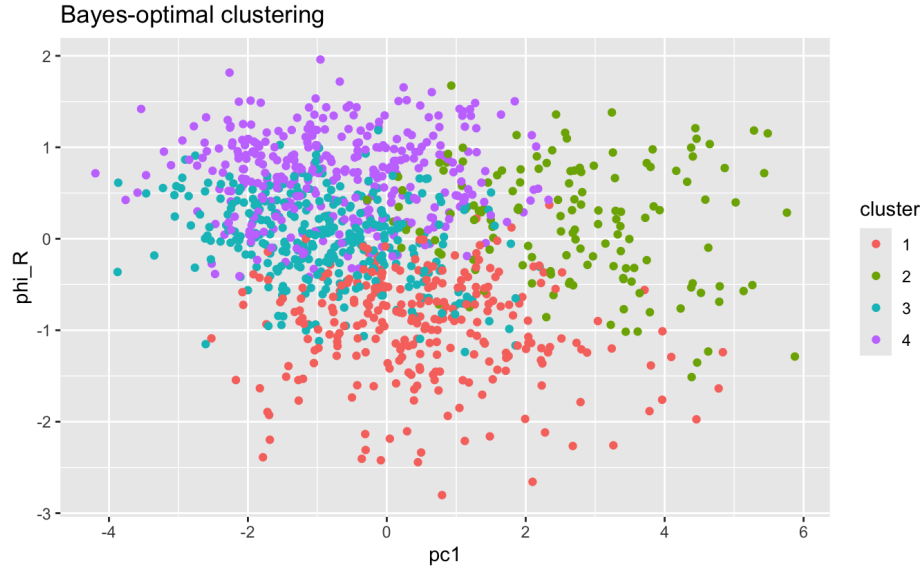


Figure 9: Bayes-optimal k-means point estimate of cluster assignments based on random effect vectors  $\theta_i$ . pc1 refers to the first principal component vector computed with the posterior means of the dynamics model random effects.

To illustrate the uncertainty quantification produced by equation (3), Figure 10 shows the probabilities of assignment to cluster 1. Although the majority of patients have probabilities very close to 0 or 1, a number of observations near the boundary with other clusters have meaningful levels of uncertainty in their assignment.

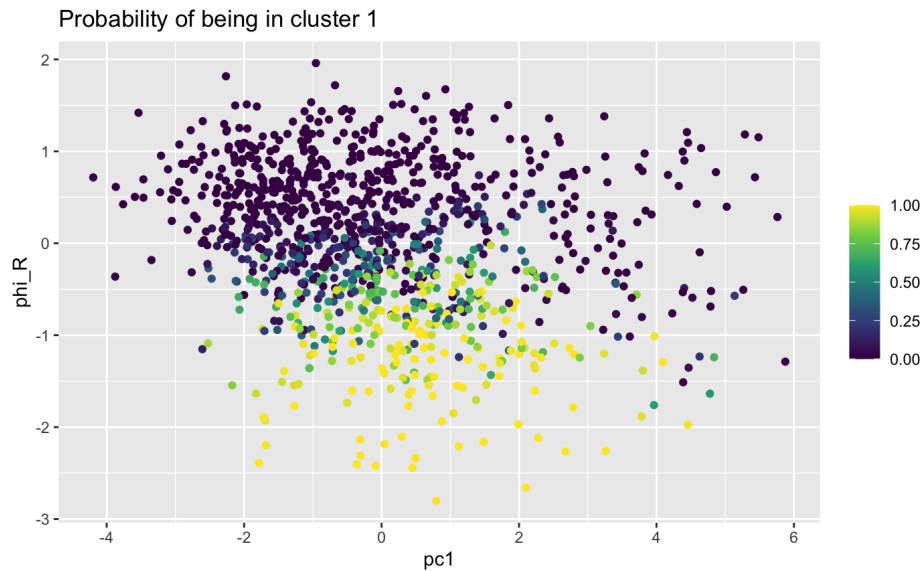


Figure 10: Posterior probability of assignment to cluster 1, computed with equation (3).

## 5.4 Relationship of cluster assignment with other variables

Given the cluster assignments learned above, we can examine how other variables of interest vary by cluster. Table 4 shows the weighted means and standard deviations of a number of demographic and clinical variables by the probability of cluster assignment. Several demographic variables appear to vary meaningfully between groups. For example, cluster 1 has a substantially higher percentage of males than the other groups, as well as the highest percentage of white patients. Examining other health variables, cluster 4 has an extremely high average BMI of 35.2, as well as an AHI of 63.7, both of which are substantially higher than those of clusters 1-3. The total amount of sleep appears reasonably similar across clusters, but the portion of that sleep spent in REM vs. non-REM differs substantially. In particular, cluster 2 has well under an hour of REM sleep on average, aligning with the highly disturbed sleep indicated by the cluster 2 center in Table 3. Finally, Table 4 shows the average scores for Pathfinder and BSRT for each group. Although these generally appear fairly similar, clusters 2 and 4 have the worst two average scores on both tests.

	Cluster 1	Cluster 2	Cluster 3	Cluster 4
Age	51.8 (13.3)	52.7 (11.1)	50.5 (12.2)	51.9 (11.8)
Fraction male	0.79	0.64	0.54	0.66
Fraction white	0.82	0.77	0.73	0.74
BMI	29.8 (5.4)	31.2 (6.2)	31.5 (6.8)	35.2 (7.9)
AHI	31.2 (17.4)	38.0 (22.1)	23.4 (10.2)	63.7 (23.7)
Hours asleep	6.26 (1.08)	6.26 (1.02)	6.43 (1.07)	6.28 (1.11)
Hours in REM sleep	1.18 (0.47)	0.86 (0.44)	1.31 (0.48)	1.04 (0.52)
Hours in non-REM sleep	5.07 (0.90)	5.41 (0.90)	5.12 (0.87)	5.25 (0.97)
Pathfinder	24.1 (7.0)	24.4 (5.8)	24.3 (6.2)	25.0 (7.1)
BSRT	50.2 (9.2)	49.0 (9.1)	50.4 (9.0)	49.2 (9.3)

Table 4: Weighted means and standard deviations of demographic and PSG variables by cluster assignment. The weights used are the posterior probabilities of assignment to each cluster.

To illustrate that random effects in our model and the clusters they produce can generate insights missed by a simple AHI approach, Table 5 shows the results of two linear regressions. The first regresses the BSRT score on the cluster label, age, and sex, while the second regresses BSRT score on AHI, age, and sex. Sex and age are found to be significant in both models, with higher age and being male associated with poorer performance. In model 1, cluster 1 has a significantly better score than reference cluster 4. However, despite the variation in AHI between the groups and the fact that group 4 has by far the highest AHI, in model 2 the coefficient for AHI is not significant at a significance level of 0.05, suggesting that there may be more to the story when relating OSA severity to a cognitive outcome like BSRT. One aspect of this is that while cluster 1 does not have the lowest AHI, it does have the lowest average  $\phi_R$ , suggesting that the rate of events may matter more in REM sleep than non-REM. Note that group 3 has the lowest AHI and the lowest average  $\phi_N$ , but does not have significantly better performance than group 4 in model 1. Similarly, while cluster 2 also

has substantially lower AHI than cluster 4, it also does not differ significantly in BSRT, and its coefficient has a negative point estimate. One interpretation of these results is that the higher AHI of cluster 4 is balanced by cluster 2’s more highly disrupted sleep, which suggests that examining OSA event occurrences and sleep dynamics together as our model does is important for understanding drivers of symptom severity.

		Estimate	Std. Error	t value	Pr(> t )
Regression 1	Intercept	62.78	1.26	49.76	<b>0.00</b>
	cluster1	1.55	0.69	2.24	<b>0.03</b>
	cluster2	-0.50	0.85	-0.60	0.55
	cluster3	0.36	0.66	0.55	0.58
	age	-0.21	0.02	-9.82	<b>0.00</b>
	sexMale	-4.06	0.56	-7.28	<b>0.00</b>
Regression 2	Intercept	63.74	1.25	51.03	<b>0.00</b>
	AHI	-0.02	0.01	-1.83	0.07
	age	-0.21	0.02	-9.80	<b>0.00</b>
	sexMale	-3.76	0.55	-6.89	<b>0.00</b>

Table 5: Results from linear regression models for BSRT score on cluster with reference level 4 (model 1) and AHI (model 2), both after accounting for age and sex. At a significance level of 0.05, model 1 finds a significant difference in BSRT score between clusters 4 and 1, but model 2 does not find a significant relationship between BSRT score and AHI.

## 5.5 Alternate clustering based on simple summary statistics

Examining the AHI and time values in each sleep stage in Table 4, it appears that these basic summary statistics vary by cluster. This suggests that despite the lower performance of the simple clustering of these variables in our simulations in Section 4, they may also give useful insight here. To explore this, we again grouped patients using the loss function of K-means with  $k = 4$ , but this time using REM AHI, non-REM AHI, time in REM, and time in non-REM as input variables. The estimated cluster centers are shown in Table 6. Cluster 1 has the lowest AHI in each sleep stage and the longest time spent in REM, while cluster 4 has the highest AHI values but the least time spent in REM.

	REM AHI	non-REM AHI	time in REM	time in non-REM
Cluster 1	29.2	23.9	1.22	5.07
Cluster 2	41.6	59.5	1.08	5.24
Cluster 3	64.9	36.1	1.16	5.22
Cluster 4	78.0	83.3	0.90	5.32

Table 6: Estimated cluster centers based on K-means loss with REM AHI, non-REM AHI, time in REM, and time in non-REM as input data.

To get a sense of how these clusters compare with those estimated using our model random effects, Figure 11 shows the cluster assignments visualized on the same axes of Figure 9. Observe that clusters 1,

3, and 4 have a pattern similar to before along the  $\phi_R$  axis, but now all four clusters are spread widely over the horizontal axis, indicating that these new clusters do not capture the variation in sleep dynamics that was captured by our model random effects.

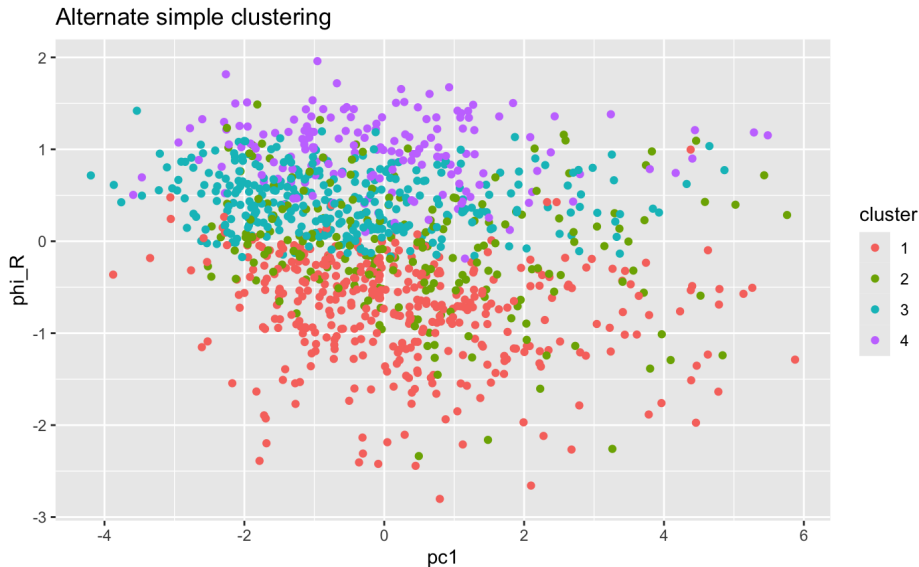


Figure 11: Cluster assignments computed using the K-means algorithm with REM AHI, non-REM AHI, time in REM, and time in non-REM as input variables, plotted on the same axes from Figure 9.

Finally, in Table 7, we examine the differences in the BSRT scores among these alternate groups. Setting cluster 4 as the reference, we find that after controlling for sex and age, patients in cluster 1 have a significantly higher expected BSRT score at a significance level of 0.05. Taken together, the above results suggest that in practice, simple summary statistics such as time in each sleep stage and stage-specific AHI can help give complementary insights to those generated by our model. More broadly, examining how other variables differ by the clusters generated by our model’s random effects can help reveal other variables that could be key to better understanding sleep differences among OSA patients.

		Estimate	Std. Error	t value	Pr(> t )
Regression 3	Intercept	62.11	1.36	45.81	<b>0.00</b>
	cluster1	1.79	0.80	2.23	<b>0.03</b>
	cluster2	1.74	0.91	1.92	0.06
	cluster3	0.63	0.84	0.76	0.45
	age	-0.21	0.02	-9.75	<b>0.00</b>
	sexMale	-3.94	0.58	-6.84	<b>0.00</b>

Table 7: Results for a linear regression of BSRT score on alternate cluster labels with reference level 4, after accounting for age and sex.

## 6 Discussion

In this work, we investigated the heterogeneity in sleep stage dynamics and stage-specific rates of apnea and hypopnea events in OSA patients by analyzing data from the APPLES study, which generated several novel insights. We found that for the average patient, having an OSA event during a given epoch increases the probability of awakening or changing sleep stages in the following epoch, although both the baseline probabilities and the magnitude of this change vary substantially among patients. Also, for the average patient, the expected wait time between OSA events is substantially shorter during REM sleep than during non-REM, although again there is significant patient variation in rates. By modeling the covariance of our model’s random effects, we revealed that during REM sleep, patient baseline rates of transitions to Awake or non-REM are positively correlated with one another, as well as being correlated with greater impact of OSA events on these transitions, while during non-REM sleep, baseline rates of transitions to REM or Awake are negatively correlated with the corresponding shifts due to events. Finally, we clustered patients into four interpretable groups based on their random effects. This revealed that other demographic and health variables, such as age, sex, and BMI, vary significantly by event rates and sleep dynamics. Turning to the cognitive performance measure BSRT, we determined that relative to group 4, which had the highest average AHI, cluster 1 had significantly better BSRT scores after correcting for age and sex. This result was noteworthy because, while cluster 1 had the lowest rate of events during REM sleep, it did not have the lowest overall AHI, supporting the hypothesis that events in REM sleep may be particularly harmful to cognitive outcomes. In contrast to our clustering approach, a regression of BSRT on AHI directly did not yield a significant association after correcting for sex and age, further emphasizing the limitations of an AHI-based analysis.

To accomplish the above, we developed a hierarchical Bayesian modeling approach for analyzing PSG data. We model both OSA event rates and sleep stage dynamics jointly, including important parameters to allow patient-specific effects of event occurrences on subsequent dynamics. We modeled the ten patient-level random effects controlling variation in these dynamics and event rates using a multivariate Gaussian distribution with factor-model covariance, thus allowing insights into shared characteristics in patient profiles. Then, to summarize patients based on their estimated random effects, we showed that a Bayes-optimal clustering under K-means loss can be easily computed when clustering by random effects is desired. This clustering result, along with the associated uncertainty quantification we propose, may be of independent interest to readers, as it generalizes to any setting where one would like to cluster observations by random effects estimated using a Bayesian model. In simulations, we showed that our inferences are robust to model misspecification and that our clustering approach captures variation missed by a simpler clustering approach using only summary statistics of event rates and sleep architecture.

There are a number of promising directions to build upon this work. From a modeling perspective, both the inter-event time and dynamics models could be generalized for greater flexibility. For example, both the fixed and random effects for transitions between sleep stages could be allowed to change as a function of time, reflecting that sleep dynamics are likely to differ between the beginning and end of the night. Similarly, the rates of event occurrences during REM and non-REM sleep could vary over time. In addition, distributions other than the Exponential could be investigated to relax the memorylessness property for the inter-event times; for example, the Weibull distribution could be a more flexible alternative. All of these proposed directions would substantially complicate the posterior sampling, so the development of efficient sampling approaches would be a key part of this research. A separate direction for future work is to extend our results for clustering based on posterior samples of Bayesian model parameters. For example, loss functions other than K-means may be desirable in different situations; it would be interesting and useful to explore approaches for Bayes-optimal clustering in these more general settings. Finally, our approach could be applied to additional data sets to answer questions we did not address here. For example, while we considered only diagnostic PSG data for OSA patients, it would be interesting to explore how sleep stage dynamics parameters vary between OSA patients and healthy volunteers, as well as how they change for OSA patients in response to treatment, for example by a CPAP machine.

## 7 Appendix

### 7.1 Proof of Proposition 3.1

Observe that, letting all expectations be over the posterior distribution  $\pi_{post}$ , we have

$$\begin{aligned}
(\hat{c}, \hat{b}) &= \arg \min_{c:|C|=K, b \in \mathbb{R}^{K \times d}} \sum_{k=1}^K \sum_{i \in C_k} \mathbb{E} [|\theta_i - b_k|^2] \\
&= \arg \min_{c:|C|=K, b \in \mathbb{R}^{K \times d}} \sum_{k=1}^K \sum_{i \in C_k} \mathbb{E} [ |(\theta_i - \mathbb{E}[\theta_i]) + (\mathbb{E}[\theta_i] - b_k)|^2 ] \\
&= \arg \min_{c:|C|=K, b \in \mathbb{R}^{K \times d}} \sum_{k=1}^K \sum_{i \in C_k} \mathbb{E} [ |\theta_i - \mathbb{E}[\theta_i]|^2 + \mathbb{E}[(\theta_i - \mathbb{E}[\theta_i])^T (\mathbb{E}[\theta_i] - b_k)] + \mathbb{E}[|\mathbb{E}[\theta_i] - b_k|^2] ] \\
&= \arg \min_{c:|C|=K, b \in \mathbb{R}^{K \times d}} \sum_{k=1}^K \sum_{i \in C_k} |\mathbb{E}[\theta_i] - b_k|^2
\end{aligned}$$

where we have used that in the second-to-last line, the first term does not depend on  $(c, b)$ , the second term is equal to zero, and the outer expectation in the third term can be dropped.  $\square$

## 8 Acknowledgments

The authors gratefully acknowledge funding from the National Institutes of Health (NIH) grant R01ES035625, the Office of Naval Research (ONR) grant N00014-21-1-2510, and Merck & Co., Inc., through its support for the Merck BARDS Academic Collaboration. The authors also acknowledge the Duke Compute Cluster for computational time and Surya Tokdar for helpful discussions.

## References

- AASM (1999). Sleep-related breathing disorders in adults: recommendations for syndrome definition and measurement techniques in clinical research. *Sleep* 22, 667–689.
- Aurora, R. N., C. Crainiceanu, D. J. Gottlieb, J. S. Kim, and N. M. Punjabi (2018). Obstructive sleep apnea during REM sleep and cardiovascular disease. *American journal of respiratory and critical care medicine* 197(5), 653–660.
- Bianchi, M. T., S. S. Cash, J. Mietus, C.-K. Peng, and R. Thomas (2010). Obstructive sleep apnea alters sleep stage transition dynamics. *PLoS One* 5(6), e11356.
- Bizzotto, R., S. Zamuner, G. De Nicolao, M. O. Karlsson, and R. Gomeni (2010). Multinomial logistic estimation of Markov-chain models for modeling sleep architecture in primary insomnia patients. *Journal of pharmacokinetics and pharmacodynamics* 37, 137–155.
- Buschke, H. (1973). Selective reminding for analysis of memory and learning. *Journal of Verbal Learning and Verbal Behavior* 12(5), 543–550.
- Carpenter, B., A. Gelman, M. D. Hoffman, D. Lee, B. Goodrich, M. Betancourt, M. Brubaker, J. Guo, P. Li, and A. Riddell (2017). Stan: A probabilistic programming language. *Journal of Statistical Software* 76(1).
- Drager, L. F., S. M. Togeiro, V. Y. Polotsky, and G. Lorenzi-Filho (2013). Obstructive sleep apnea: a cardiometabolic risk in obesity and the metabolic syndrome. *Journal of the American College of Cardiology* 62(7), 569–576.
- Eckert, D. J., D. P. White, A. S. Jordan, A. Malhotra, and A. Wellman (2013). Defining phenotypic causes of obstructive sleep apnea. identification of novel therapeutic targets. *American journal of respiratory and critical care medicine* 188(8), 996–1004.
- Edwards, B. A., S. Redline, S. A. Sands, and R. L. Owens (2019). More than the sum of the respiratory

- events: personalized medicine approaches for obstructive sleep apnea. *American journal of respiratory and critical care medicine* 200(6), 691–703.
- Gagnadoux, F., M. Le Vaillant, A. Paris, T. Pigeanne, L. Leclair-Visonneau, A. Bizieux-Thaminy, C. Alizon, M.-P. Humeau, X.-L. Nguyen, B. Rouault, et al. (2016). Relationship between osa clinical phenotypes and cpap treatment outcomes. *Chest* 149(1), 288–290.
- Hermans, L. W., I. A. Huijben, H. van Gorp, T. R. Leufkens, P. Fonseca, S. Overeem, and M. M. van Gilst (2022). Representations of temporal sleep dynamics: Review and synthesis of the literature. *Sleep Medicine Reviews* 63, 101611.
- Jokic, R., A. Klimaszewski, M. Crossley, G. Sridhar, and M. F. Fitzpatrick (1999). Positional treatment vs continuous positive airway pressure in patients with positional obstructive sleep apnea syndrome. *Chest* 115(3), 771–781.
- Kaplan, E. L. and P. Meier (1958). Nonparametric estimation from incomplete observations. *Journal of the American statistical association* 53(282), 457–481.
- Kapur, V. K., H. E. Resnick, D. J. Gottlieb, and S. H. H. S. Group (2008). Sleep disordered breathing and hypertension: does self-reported sleepiness modify the association? *Sleep* 31(8), 1127–1132.
- Karlsson, M. O., R. C. Schoemaker, B. Kemp, A. F. Cohen, J. M. van Gerven, B. Tuk, C. C. Peck, and M. Danhof (2000). A pharmacodynamic Markov mixed-effect model for the effect of temazepam on sleep. *Clinical Pharmacology & Therapeutics* 68(2), 175–188.
- Kjellsson, M. C., D. Ouellet, B. Corrigan, and M. O. Karlsson (2011). Modeling sleep data for a new drug in development using Markov mixed-effects models. *Pharmaceutical research* 28, 2610–2627.
- Klerman, E. B., W. Wang, J. F. Duffy, D.-J. Dijk, C. A. Czeisler, and R. E. Kronauer (2013). Survival analysis indicates that age-related decline in sleep continuity occurs exclusively during NREM sleep. *Neurobiology of aging* 34(1), 309–318.
- Koch, H., L. D. Schneider, L. A. Finn, E. B. Leary, P. E. Peppard, E. Hagen, H. B. D. Sorensen, P. Jennum, and E. Mignot (2017). Breathing disturbances without hypoxia are associated with objective sleepiness in sleep apnea. *Sleep* 40(11), zsx152.
- Kushida, C. A., D. A. Nichols, S. F. Quan, J. L. Goodwin, D. P. White, D. J. Gottlieb, J. K. Walsh, P. K. Schweitzer, C. Guilleminault, R. D. Simon, et al. (2006). The apnea positive pressure long-term efficacy study (APPLES): Rationale, design, methods, and procedures. *Journal of Clinical Sleep Medicine* 2(03), 288–300.

- Lloyd, S. (1982). Least squares quantization in pcm. *IEEE transactions on information theory* 28(2), 129–137.
- Mantel, N. et al. (1966). Evaluation of survival data and two new rank order statistics arising in its consideration. *Cancer Chemother Rep* 50(3), 163–170.
- Mathur, S. and J. Sutton (2017). Personalized medicine could transform healthcare. *Biomedical reports* 7(1), 3–5.
- Mokhlesi, B., L. A. Finn, E. W. Hagen, T. Young, K. M. Hla, E. Van Cauter, and P. E. Peppard (2014). Obstructive sleep apnea during REM sleep and hypertension. results of the Wisconsin sleep cohort. *American journal of respiratory and critical care medicine* 190(10), 1158–1167.
- Norman, R. G., M. A. Scott, I. Ayappa, J. A. Walsleben, and D. M. Rapoport (2006). Sleep continuity measured by survival curve analysis. *Sleep* 29(12), 1625–1631.
- Osman, A. M., S. G. Carter, J. C. Carberry, and D. J. Eckert (2018). Obstructive sleep apnea: current perspectives. *Nature and science of sleep*, 21–34.
- Partington, J. E. and R. G. Leiter (1949). Partington’s pathways test. *Psychological Service Center Journal*.
- Pase, M. P., S. Harrison, J. R. Misialek, C. E. Kline, M. Cavuoto, A.-A. Baril, S. Yiallourou, A. Bisson, D. Himali, Y. Leng, et al. (2023). Sleep architecture, obstructive sleep apnea, and cognitive function in adults. *JAMA network open* 6(7), e2325152–e2325152.
- Peever, J. and P. M. Fuller (2017). The biology of REM sleep. *Current biology* 27(22), R1237–R1248.
- Poworoznek, E., N. Anceschi, F. Ferrari, and D. Dunson (2021). Efficiently resolving rotational ambiguity in Bayesian matrix sampling with matching. *arXiv preprint arXiv:2107.13783*.
- Quan, S. F., C. S. Chan, W. C. Dement, A. Gevins, J. L. Goodwin, D. J. Gottlieb, S. Green, C. Guilleminault, M. Hirshkowitz, P. R. Hyde, et al. (2011). The association between obstructive sleep apnea and neurocognitive performance—the apnea positive pressure long-term efficacy study (APPLES). *Sleep* 34(3), 303–314.
- R Core Team (2023). *R: A Language and Environment for Statistical Computing*. Vienna, Austria: R Foundation for Statistical Computing.
- Rechtschaffen, A. and A. Kales (1968). A manual of standardized terminology, techniques and scoring system for sleep stages of human subjects. Washington DC: Public Health Service. *US Government Printing Office*.

- Rigon, T., A. H. Herring, and D. B. Dunson (2023). A generalized Bayes framework for probabilistic clustering. *Biometrika* 110(3), 559–578.
- Rundo, J. V. and R. Downey III (2019). Polysomnography. *Handbook of clinical neurology* 160, 381–392.
- Sankari, A., S. Pranathiageswaran, S. Maresh, A. M. Hosni, and M. S. Badr (2017). Characteristics and consequences of non-apneic respiratory events during sleep. *Sleep* 40(1), zsw024.
- Senaratna, C. V., J. L. Perret, C. J. Lodge, A. J. Lowe, B. E. Campbell, M. C. Matheson, G. S. Hamilton, and S. C. Dharmage (2017). Prevalence of obstructive sleep apnea in the general population: a systematic review. *Sleep medicine reviews* 34, 70–81.
- Varga, A. W. and B. Mokhlesi (2019). REM obstructive sleep apnea: risk for adverse health outcomes and novel treatments. *Sleep and Breathing* 23, 413–423.
- Walia, H. K., H. Li, M. Rueschman, D. L. Bhatt, S. R. Patel, S. F. Quan, D. J. Gottlieb, N. M. Punjabi, S. Redline, and R. Mehra (2014). Association of severe obstructive sleep apnea and elevated blood pressure despite antihypertensive medication use. *Journal of Clinical Sleep Medicine* 10(8), 835–843.
- Weaver, E. M., B. T. Woodson, and D. L. Steward (2005). Polysomnography indexes are discordant with quality of life, symptoms, and reaction times in sleep apnea patients. *Otolaryngology—Head and Neck Surgery* 132(2), 255–262.
- Wheaton, A. G., G. S. Perry, D. P. Chapman, and J. B. Croft (2012). Sleep disordered breathing and depression among us adults: National health and nutrition examination survey, 2005-2008. *Sleep* 35(4), 461–467.
- Yetton, B. D., E. A. McDevitt, N. Cellini, C. Shelton, and S. C. Mednick (2018). Quantifying sleep architecture dynamics and individual differences using big data and Bayesian networks. *PLoS one* 13(4), e0194604.
- Zhang, G.-Q., L. Cui, R. Mueller, S. Tao, M. Kim, M. Rueschman, S. Mariani, D. Mobley, and S. Redline (2018). The national sleep research resource: towards a sleep data commons. *Journal of the American Medical Informatics Association* 25(10), 1351–1358.
- Zinchuk, A. V., M. J. Gentry, J. Concato, and H. K. Yaggi (2017). Phenotypes in obstructive sleep apnea: a definition, examples and evolution of approaches. *Sleep medicine reviews* 35, 113–123.

## 9 Supplementary Information

### 9.1 Alternate clustering methods

#### 9.1.1 Point estimation using the formulation in equation (2)

For comparison to the clustering point estimate computed in the main paper based on equation (1), we compute an estimate based on equation (2), where we optimize only over cluster assignments, not simultaneously estimating the cluster centers. Recall the form of equation (2):

$$\hat{c}' = \arg \min_{c:|C|=K} \sum_{k=1}^K \sum_{i \in C_k} \mathbb{E}_{\pi_{post}} [\|\theta_i - \bar{\theta}_k\|^2], \quad (\text{S1})$$

where  $\bar{\theta}_k$  is the mean of the observations in cluster  $k$ . Observe that to compute  $\hat{c}'$  in the above given  $m$  posterior samples of each  $\theta_i$  vector, we can again apply standard K-means code, but using  $\tilde{\theta}_i \in \mathbb{R}^{pm}$  for  $i = 1, \dots, n$  as input data, where we define  $\tilde{\theta}_i$  as all  $m$  posterior samples of  $\theta_i \in \mathbb{R}^p$  concatenated together into a single vector. To see why, observe that using posterior means to estimate the expectations in (S1), the loss function becomes

$$\begin{aligned} \sum_{k=1}^K \sum_{i \in C_k} \sum_{j=1}^m \|\theta_{ij} - \bar{\theta}_{kj}\|^2 &= \sum_{k=1}^K \sum_{i \in C_k} \sum_{j=1}^m \sum_{l=1}^p (\theta_{ijl} - \bar{\theta}_{kjl})^2 \\ &= \sum_{k=1}^K \sum_{i \in C_k} \|\tilde{\theta}_i - \bar{\theta}_k\|^2, \end{aligned}$$

i.e., the standard K-means loss function applied to vectors  $\tilde{\theta}_1, \dots, \tilde{\theta}_n$ . Implementing this in R (R Core Team, 2023), we get the estimated cluster assignments shown in Figure 12 below, visualized on the same axes as in Figure 9 of the paper. Ignoring label switching, the clusters appear very similar to the ones we computed using equation (1). The adjusted Rand index between the two clusterings is 0.998, indicating extremely strong agreement. Thus, for this setting, the two estimates are almost interchangeable. We suggest a more full comparison of the two approaches as an interesting direction for future work.

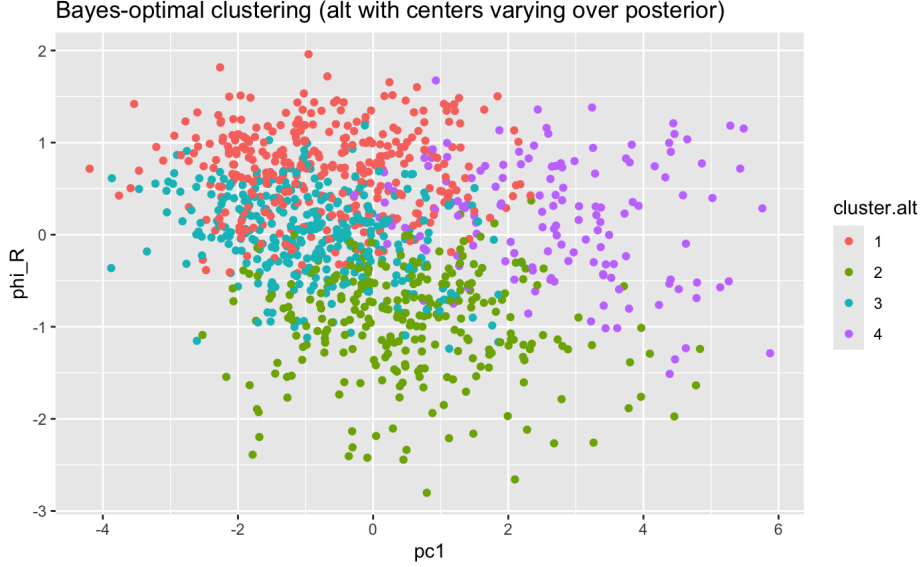


Figure 12: Bayes-optimal k-means point estimate of cluster assignments based on random effect vectors  $\theta_i$  using the formulation in (S1). pc1 refers to the first principal component vector computed with the posterior means of the dynamics model random effects.

### 9.1.2 Alternate approaches for clustering uncertainty quantification

#### (1) Applying k-means to each posterior sample

One conceptually simple approach to characterizing uncertainty in the optimal clusters and centers is to simply run the k-means algorithm separately on each posterior sample, generating  $m$  posterior samples of the optimal clustering.

$$(\tilde{c}_j, \tilde{b}_j) = \arg \min_{c:|C|=K, b \in \mathbb{R}^{K \times d}} \sum_{k=1}^K \sum_{i \in C_k} \|\theta_{ij} - b_{kj}\|^2, \quad j = 1, \dots, m. \quad (\text{S2})$$

While this is in some sense a natural choice, it presents two practical issues. First, relating summaries of these clusterings directly to our point estimate is nontrivial due to label-switching, so we would instead need to rely on related summaries like pairwise co-clustering probabilities. Second, and more fundamentally, the relationship between the distribution of the arg mins in (S2) and the arg min of the expected loss in equation (1) is also not straightforward; e.g., our point estimate using equation (1) may be assigned a posterior probability of 0 in (S2), while cluster assignments sampled in (S2) may be extremely suboptimal in equation (1), making it difficult to interpret summaries this method produces.

Despite these difficulties, we implemented this approach, and we summarize the results below in Figure 13. Pairwise co-clustering probabilities for all patients are visualized in the left panel of the figure, with dark red representing a probability of 1, and light yellow representing 0. The observations are ordered so that the

observed block-diagonal pattern corresponds to observations whose point estimates were cluster 1, 2, 3, and 4. Clearly, there is some general agreement between the co-clustering probabilities and the point estimate; however, there are also a number of patients whose co-clustering probabilities with others in their cluster point estimate are quite low. Since there is no reliable notion of cluster locations across samples now, to summarize the probabilities of assignment to “Cluster 1,” we computed co-clustering probabilities with the patient whose  $\theta_i$  posterior mean was the closest to our cluster 1 center point estimate. Doing so yields a similar distribution of probabilities as in Figure 10 in the paper; however, it is misleading to give the values the same interpretation, as they are computed in fundamentally different ways.

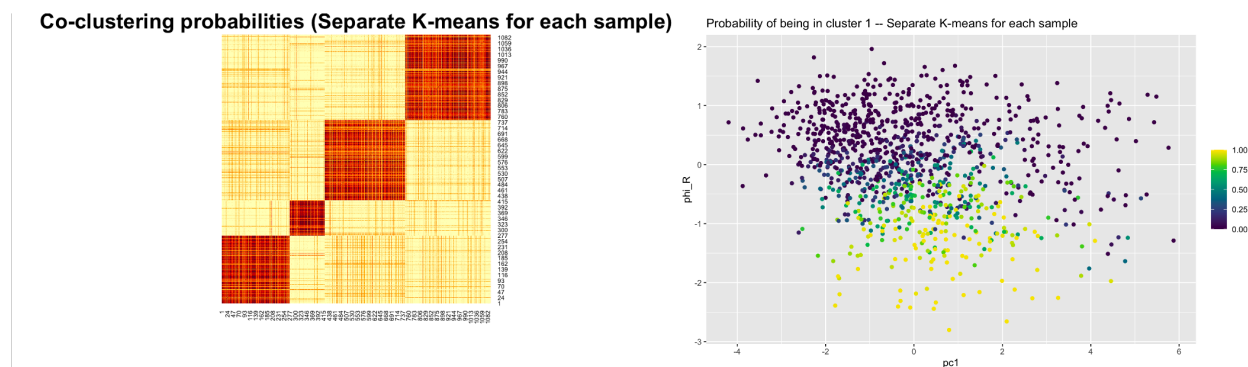


Figure 13: Co-clustering probabilities (left) and probabilities of being co-clustered with the individual closest to the cluster 1 center point estimate (right) for the distribution of clusterings learned by applying K-means to each of the 10,000 posterior samples of  $\theta_1, \dots, \theta_n$ .

Finally, to compare this learned distribution of clusterings to our point estimate directly, we use the adjusted Rand index between each of the 10,000 cluster estimates and our point estimate. This results in a mean ARI of 0.58, standard deviation 0.05, and a range of 0.28 to 0.71. This suggests meaningful disagreement on average, and none of the individual sample clusterings are equivalent to the point estimate.

## (2) Generalized Bayesian inference based on Rigon et al. (2023)

A second approach for loss-based clustering uncertainty quantification is the generalized Bayes approach proposed by Rigon et al. (2023). If we ignore patient-level uncertainty and treat each  $\hat{\theta}_i$  as observed, we can sample from a Gibbs posterior representing rational posterior beliefs about the optimal clustering in terms of expected k-means loss over the unknown population distribution of  $\theta_i$ , again yielding a distribution of clusterings. In addition to the difficulties in summarizing such a distribution mentioned above, this Gibbs posterior critically depends on a tuning parameter  $\lambda$ ; at extreme choices of  $\lambda$ , the clustering distribution can collapse to a point mass at a single partition, or can be flat over all possible partitions. While Rigon et al. (2023) propose an approach for choosing a reasonable  $\lambda$  for k-means, interpretability of the resulting probabilities is again a concern.

We also implement this approach for comparison, using the Gibbs sampler described in [Rigon et al. \(2023\)](#) with 10,000 samples drawn. We show the same summaries as in the previous section below in [Figure 14](#). In general, agreement with our point estimate appears stronger here than in [Figure 13](#).

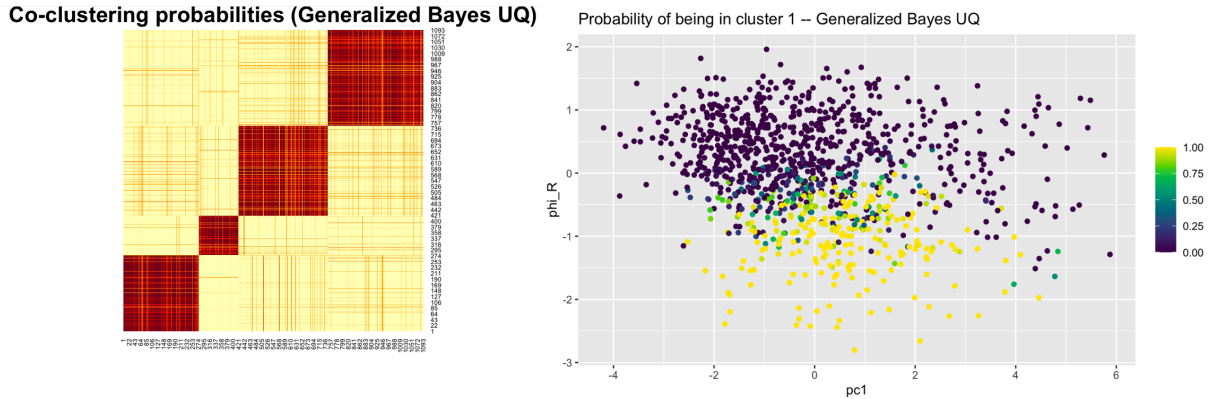


Figure 14: Co-clustering probabilities (left) and probabilities of being co-clustered with the individual closest to the cluster 1 center point estimate (right) for the Gibbs posterior of clusterings learned by applying the method of [Rigon et al. \(2023\)](#).

Computing ARI values for each sample, we get a mean of 0.76, standard deviation 0.02, and a range of 0.69 to 0.83. Thus, again we get that our point estimate has an estimated probability of zero.

## 9.2 Additional posterior predictive checks

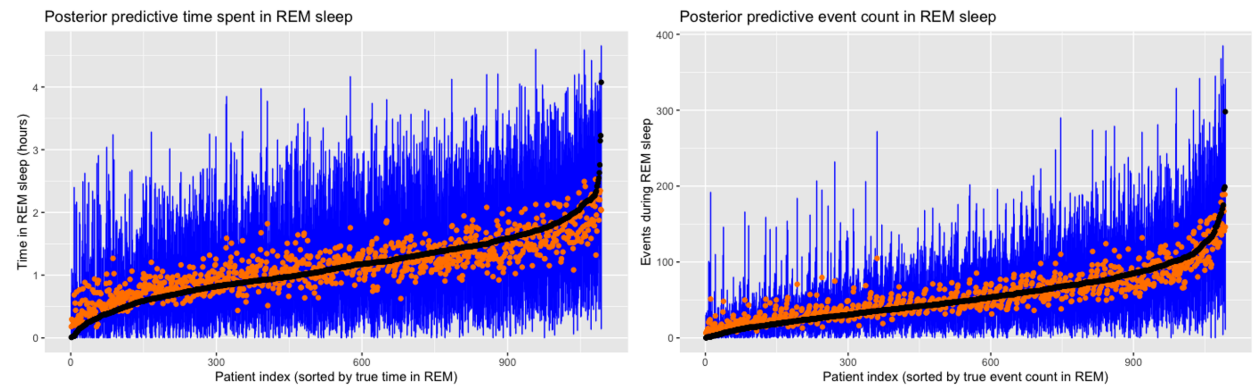


Figure 15: Posterior predictive distributions of time spent in REM sleep (left) and the number of events occurring during REM sleep (right). Black dots are observed values; orange dots are posterior predictive means; blue lines are 95% posterior predictive intervals.

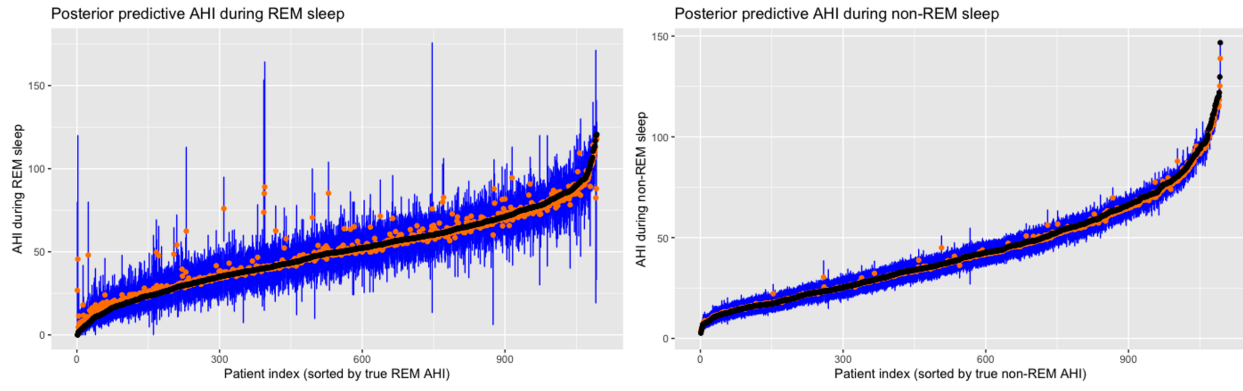


Figure 16: Posterior predictive distributions of AHI during REM sleep (left) and AHI during non-REM sleep (right). Black dots are observed values; orange dots are posterior predictive means; blue lines are 95% posterior predictive intervals.